Calibration and Validation of LCTF Camera on an Experimental Airborne Mission at Gerona and Ramos, Tarlac, Philippines

Calvo, J. S.[1,a], Paringit, E. C.[1,b], Viray, F. M.[1,c], Maestro, M. M.[1,d],
Ishida, T.[2], Namuco, S. B.[3,e], Fulgencio, L. C.[3,f]
[1]PHL-MICROSAT Project 4, Training Center for Applied Geodesy and Photogrammetry,
University of the Philippines, Diliman, Quezon City 1101, Philippines,
Email: [a]jamesalbertcalvo@gmail.com, [b]paringit@gmail.com,
[c]f.viray13@gmail.com, [d]alainmmaestro@gmail.com
[2]Department of Cosmoscience, Faculty of Science, Hokkaido University, Kita 10 Nishi 8,
Kita-ku, Sapporo, Hokkaido 060-0810, Japan,
Email: ishida.tetsu6@gmail.com
[3] PHL-MICROSAT Project 5, Institute of Environmental Science and Meteorology,
University of the Philippines, Diliman, Quezon City 1101, Philippines,
Email: [e]sbnamuco@gmail.com, [f]lcfulgencio@gmail.com

KEY WORDS: Remote sensing; Digital number; Spectral radiance; Radiometric calibration; Calibration parameters

ABSTRACT: An experimental airborne mission over an agricultural field in Gerona and Ramos, Tarlac, Philippines was carried to calibrate and validate remote sensing instruments for the Philippines' first microsatellite. Particularly, the mission aimed to calculate calibration parameters for converting Liquid Crystal Tunable Filter (LCTF) Camera spectral image band data from digital numbers (DN) to spectral radiance. The LCTF Camera was flown vicariously with another airborne imaging spectrometer, CASI for comparison. The two sensors were mounted simultaneously on a CESSNA 206 aircraft with an average flying speed of 60 m/s at an altitude ranging from 550m to 600m for the airborne data acquisition collecting a total of 20,850 images, with a spatial resolution of 0.5m and image swath of 300m for the CASI images, and a spatial resolution of 0.7m and image swath of 700m for the LCTF camera images. A field spectroradiometer (FS) was used to simultaneously measure field spectral reflectance. A spectral irradiance model was used to convert data from radiance to reflectance or vice versa. The LCTF camera data was then correlated to the field spectral data in order to generate calibration parameters. Using the calibration parameters, the LCTF camera data were converted from DN to spectral radiance, and cross-validated with the CASI and FS data using linear regression. The validation with the CASI data displayed a correlation of 0.743369 for the bands at 460nm to 700nm but an inferior correlation of 0.441638 for the near-infrared (NIR) bands 720nm and 750nm. The validation with FieldSpec data displayed a correlation of 0.387419 on the lower spectra compared to the correlation of 0.2535 of the NIR bands. The results show about 35-40% difference in spectral radiance at the near-infrared bands of the calibration parameters from the LCTF camera DN data. The calibration parameters show an effectiveness when converting data acquired in the afternoon, the root-mean-square error is significantly higher (200%) when applied to data acquired in the morning.

1. INTRODUCTION

The first Earth-observation microsatellite of the Philippines, called Diwata-1, is equipped with a High Precision Telescope (HPT) for disaster monitoring, a Spaceborne Multispectral Imager (SMI) for vegetation and ocean biomass monitoring, Middle Field Camera that aids the attitude control algorithm and Wide Field Camera for weather observation (Vergel et al, 2015; Sakamoto et al, 2015). Two of these payloads, the HPT and SMI, have Liquid Crystal Tunable Filter (LCTF) as the optical filter verifying the need to develop a method of calibrating and validating the sensor.

For the experimental airborne mission, an LCTF camera manufactured by Genesia Corporation was used. The camera has a spatial resolution of 656 x 494 pixels, angle of view of 90 degrees, ground spatial distance varying depending on the altitude, and is in tunable range of 460 nm to 780 nm. The bands can be selected in 1 nm sampling interval with spectral resolution varying from 10 nm to 50 nm depending on the central wavelength. For this airborne campaign, the 11 pre-selected bands for the LCTF camera were as follows: 460 nm; 470 nm; 490 nm; 510 nm; 530 nm; 560 nm; 640 nm; 670 nm; 700 nm; 720 nm; and 750 nm. The bands were chosen to emphasize the peaks at the green, red and near-infrared wavelength regions to mimic the objective of the LCTF sensor of Diwata-1. Radiometric corrections due to sensor sensitivity and sun angle were applied to the multispectral images of the LCTF camera for a more accurate comparison to measurements obtained using a spectroradiometer, FieldSpec 4 standard-resolution (FS).

Figure 1. The (1) LCTF camera with the (2) controller and (3) power supply.

The spectroradiometer used to obtain ground reflectance measurements was manufactured by ASD Incorporated. The FieldSpec 4 standard-res model has a spectral range of 350nm to 2500 nm with a spectral resolution of 3 nm on the visible light to near infrared region and 10nm at the short-wavelength infrared range (ASD, 2015). Using Bird's Simple Spectral Model to calculate the spectral irradiance, the FS data were converted from reflectance to spectral radiance. The irradiance model takes into account direct normal irradiance due to Rayleigh scattering, aerosol scattering and absorption, water vapor absorption, ozone and mixed gas absorption, and diffuse irradiance on horizontal and inclined surfaces (Bird and Riordan, 1984). Linear regression was used to correlate the LCTF data in DN and FS data in spectral radiance to derive calibration parameters.

With the calibration parameters derived, the LCTF data were converted from digital numbers to spectral radiance. The calibration parameters were validated by testing the accuracy of the converted data to measurements obtained by another sensor, a Compact Airborne Spectographic Imager (CASI-1500). CASI is a visible light – near infrared pushbroom type sensor with a spectral range of 380 nm to 1050 nm, spectral resolution at full-width half-maximum of 3.5 nm, total field of view of 40 degrees and an instantaneous field of view of 0.49 milliradians (ITRES, 2008). Linear regression was also used for the validation of data. The criteria considered on verifying the calibration parameters were the correlation and the root-mean-square error (RMSE) of the CASI data in radiance versus the LCTF data in radiance.

2. SIMULTANEOUS DATA ACQUISITION

The airborne campaign was conducted at Gerona and Ramos, both are municipalities located at the province of Tarlac in the Philippines. The simultaneous data acquisition was organized and executed on April 1 and 2, 2016 from 9:00 am to 5:30 pm. The target objects for calibration and validation were selected beforehand so as to plan and perform the campaign smoothly. The CASI and LCTF camera were placed coincidentally on a CESSNA 206 aircraft that is leased to Phil-LiDar 1. Both sensors capturing spectral images at the same time and simultaneously, teams on the ground are measuring surface reflectance values of the target objects using the ASD FieldSpec.

The selected target objects were agricultural crops that are prevalent on agricultural farms and fields at Tarlac like cashew, eggplant, legumes, mahogany, mango, mung beans, onion, rice, sugarcane, sweet potato, tomato, and turnip. The target agricultural crops were divided into two, grouped according to convenience of location. The first group (eggplant, mung beans, onion, rice, sweet potato) was observed in the morning of the day one and in the afternoon of day two. While the

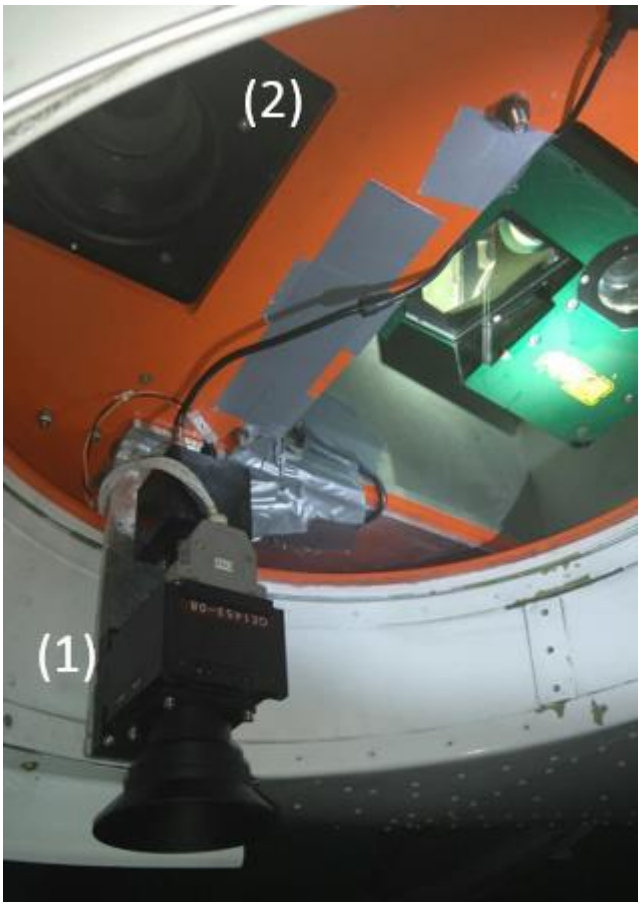

Figure 2. (1) LCTF camera and (2) CASI mounted together as seen from below a CESSNA 206.

second group (cashew, legumes, mahogany, mango, sugarcane, tomato, turnip) was observed in the afternoon of day one and in the morning of day two.

The aircraft carrying the two sensors, CASI and LCTF, was flying at an altitude varying from 550 m up to 600m with an average speed of 60 m/s. For the two-day duration of the experimental airborne campaign, a total of 20,850 images were captured covering all the designated target objects. For the FS data acquisition, 10 to 12 samples per plant type were taken for the low and intermediate growing crops while one to three samples per plant type for the high-reaching trees like mango and mahogany. All data acquired on the campaign were sorted according to acquisition time: April 1 morning data; April 1 afternoon data; April 2 morning data; and April 2 afternoon data. Data acquired between 9:00 am and 12:00 nn were classified as a morning data while those acquired between 2:00 pm and 5:30 pm were classified as afternoon data.

3. METHODOLOGY

Surface reflectance is the ratio of target object radiance and the reference panel radiance or solar irradiance (Peddle, 2001). With FS data reflectance values and spectral irradiance model, the spectral radiance values of the targets were calculated. Using the transmittance function of the LCTF camera as a filter, the FS data radiance values were tuned from ground level to LCTF camera sensor level. In the determination of LCTF camera calibration parameters, linear regression was used. The LCTF camera data in DN, with radiometric corrections for vignetting effect and sun angle, were linearly correlated to the FS data in spectral radiance (at sensor level). April 1 morning LCTF data will be compared to April 1 morning FS data, April 1 afternoon LCTF data will be compared to April 1 afternoon FS data, and so on. The calibration was executed per band in order to obtain gain and offset parameters that are unique for each of the 11 pre-selected bands of the campaign. Each data set (April 1 morning data; April 1 afternoon data; April 2 morning data; and April 2 afternoon data) has its own set of calibration parameters.

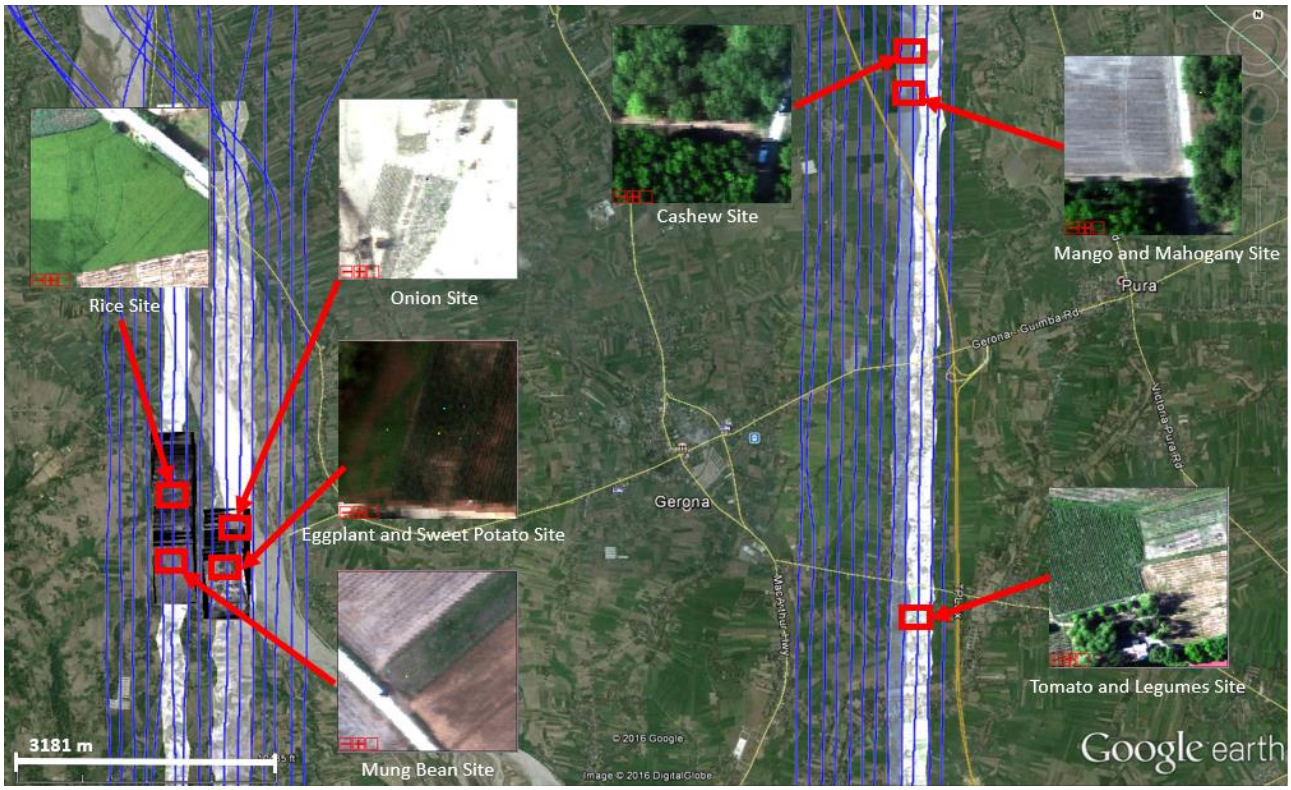

Figure 3. Overlaying the CASI and LCTF images which covers the target plants on Google earth. The blue lines show the actual flight trajectory of the aircraft carrying the two sensors.

Applying the obtained gain and offset parameters, the LCTF data were converted from DN to spectral radiance. To validate the calibration parameters, the converted LCTF data will be correlated to CASI and FS data. With radiance versus radiance comparison, the root-mean-square error was used as a criteria to express if the calibration parameters are credible. Linear regression was used for the radiance to radiance comparisons and was also executed per band. For this data validation, the comparison of data sets were paired according to acquisition time.

4. RESULTS AND DISCUSSION

The LCTF data in DN were linearly correlated to the FS data in radiance. With the comparisons executed per band, the correlation, gain and offset values obtained were unique for each band. As we can see in Figure 4, the April 1 morning and April 2 afternoon data sets generally exhibit high correlation values. For the April 1 morning data set the correlation was low on the near-infrared bands 720 nm and 750 nm while for the April 2 afternoon data set the correlation was low on the 530 nm, 560 nm and 700 nm bands. We examined the gain and offset parameters of these two data sets.

Table 1. The correlation, gain and offset parameters (unique per band) of the two data sets April 1 morning and April 2 afternoon.

Band No.	Wavelength (nm)	April 1 Morning			April 2 Afternoon		
		R^2	Gain	Offset	R^2	Gain	Offset
1	460	0.8314	50.76142	-159.929	0.7942	4.679457	-6.09499
2	470	0.8219	43.29004	-158.468	0.7614	4.826255	-16.9479
3	490	0.7367	35.21127	-185.511	0.7948	3.863988	-24.0792
4	510	0.8441	34.12969	-172.065	0.8485	5.128205	-33.92
5	530	0.8434	25.90674	-135.845	0.5153	6.127451	-73.1556
6	560	0.8207	17.88909	-94.2648	0.412	5.640158	-65.0987
7	640	0.9196	18.51852	-93.5944	0.6928	3.717472	-19.0632

8	670	0.9447	20.70393	-84.1325	0.7525	4.468275	-29.0094
9	700	0.8194	35.33569	-90.4664	0.4712	9.496676	-54.623
10	720	0.1179	107.5269	-424.516	0.8003	18.51852	-80.6593
11	750	0.0012	-555.556	4881.833	0.8742	8.53971	-14.7284

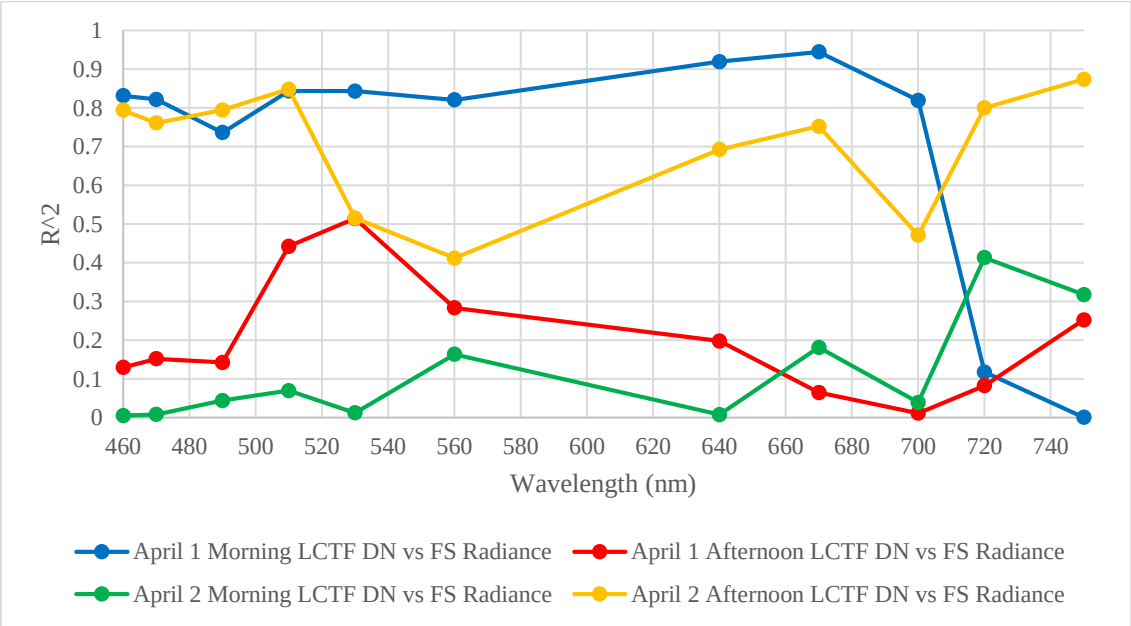

Figure 4. Linear correlation per band of LCTF DN versus FS radiance.

As can be seen in Table 1, the gain and offset for the 750 nm band are -555.556 and 4881.833, respectively. These values are very high and the gain has a negative value making the April 1 morning calibration parameters invalid. This leaves us with only one set of calibration parameters which is of the April 2 afternoon data.

With the calibration parameters of the April 2 afternoon data, the LCTF data in DN were converted to spectral radiance with W/m^2/µm as the unit of measurement. Cross-validation of the LCTF data in radiance was conducted. For the validation with CASI data, it can be seen in Figure 7 (a), that the correlations were generally high except for the 720 nm and 750 nm bands of the April 1 morning data set and the 470 nm, 490 nm, 560 nm, 720 nm, 750 nm bands of the April 1 afternoon data set, with linear correlation coefficient values 0.3606, 0.0038, 0.4102, 0.3531, 0.4183, 0.1266, and 0.1552, respectively. In Figure 5 (b), it can be seen that the data in the mornings of April 1 and April 2 advertised high values a root-mean-square error, 91.98997 W/m^2/µm up to 630.1072 W/m^2/µm while the data in the afternoons showed high RMSE values for the 750 nm band only. The RMSE values for the 460 nm to 720 nm bands of the data in the afternoons were ranging from 10.98928 W/m^2/µm to 51.19534 W/m^2/µm only.

For the validation with the FS data in radiance, the April 2 afternoon data set was not included since the calibration parameters were derived from it. Figure 8 (a) shows a low correlation between the LCTF data calibrated to radiance and the FS data. Only the April 1 morning data set displayed a high correlation coefficient of 0.83 to 0.93 from the 460 nm to 700 nm bands while the 720 nm and 750 nm bands and all bands of the April 1 afternoon and April 2 morning data sets exhibited a non-correlation with correlation coefficient values of 0.43 and lower. Figure 6 (b) shows the RMSE plots for the validation with FS data in radiance. Similar to the validation with CASI, the data in the mornings exhibited higher RMSE values. In the April 1 morning and April 2 morning data sets, the RMSE values range from 71.9617 W/m^2/µm up to 310.5751 W/m^2/µm. On the other hand for the April 1 afternoon data, only the 720 nm and 750 nm bands have high RMSE values of 87.6971 W/m^2/µm and 87.87622 W/m^2/µm, respectively. The lower spectra bands of the April 1 afternoon data have lower RMSE values ranging from 16.06883 W/m^2/µm to 61.96691 W/m^2/µm.

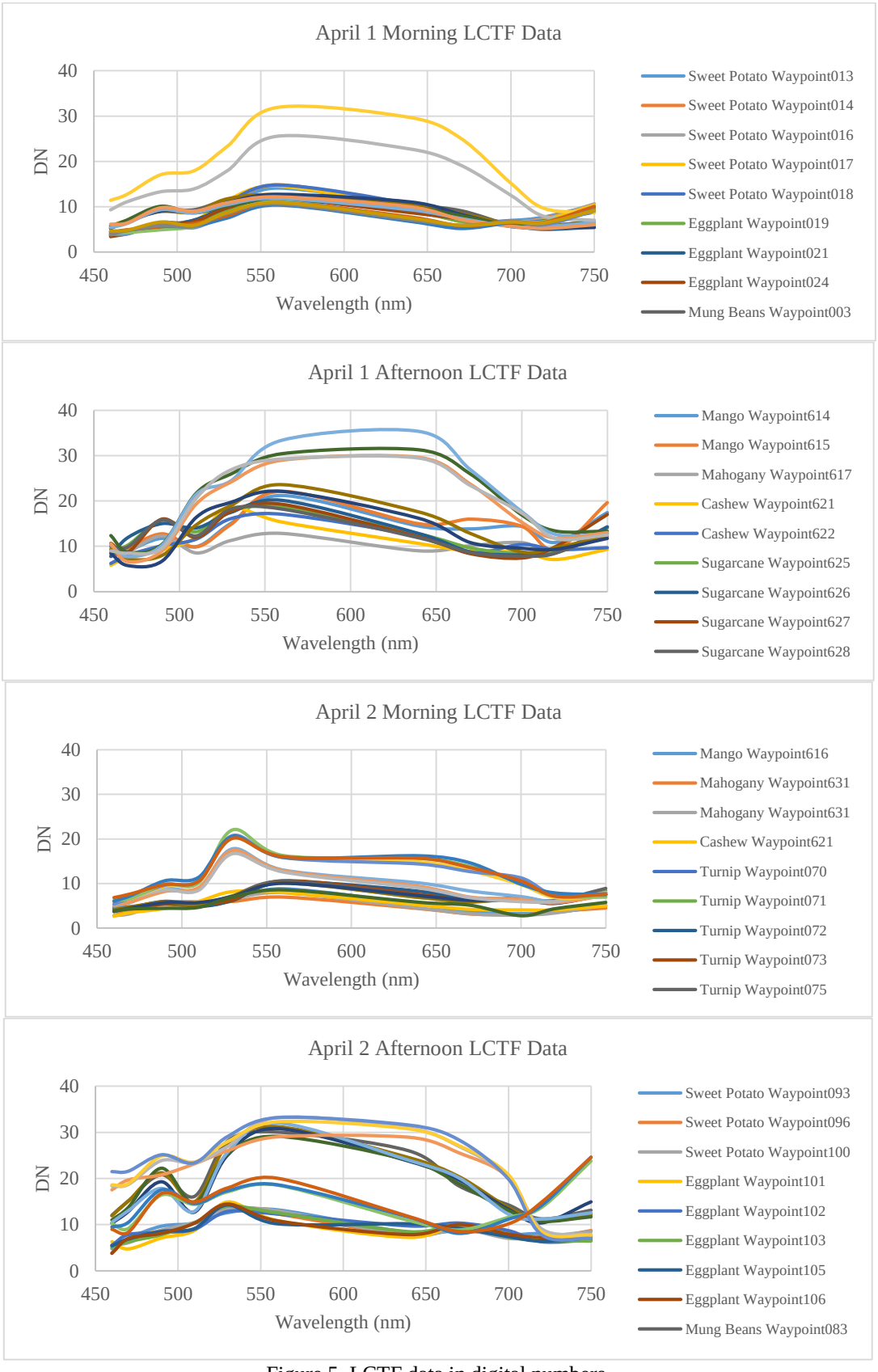

Figure 5. LCTF data in digital numbers.

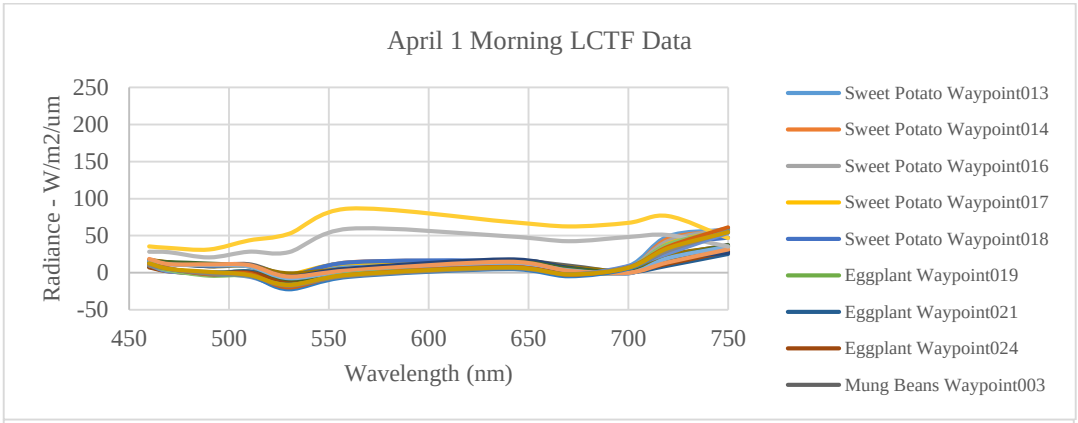
April 1 Morning LCTF Data
Radiance - W/m2/um
250
200
150
100
50
0
-50
450
500
550
600
650
700
750
Wavelength (nm)
Sweet Potato Waypoint013
Sweet Potato Waypoint014
Sweet Potato Waypoint016
Sweet Potato Waypoint017
Sweet Potato Waypoint018
Eggplant Waypoint019
Eggplant Waypoint021
Eggplant Waypoint024
Mung Beans Waypoint003

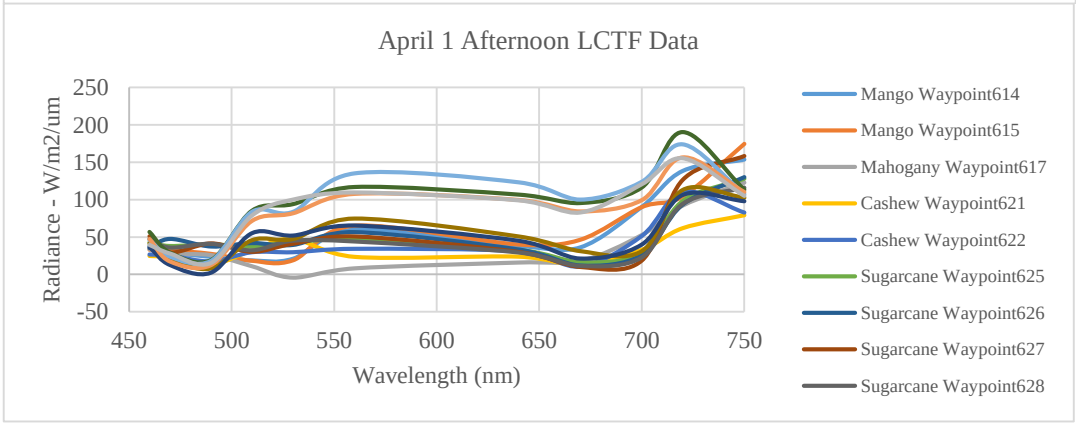
April 1 Afternoon LCTF Data
Radiance - W/m2/um
250
200
150
100
50
0
-50
450
500
550
600
650
700
750
Wavelength (nm)
Mango Waypoint614
Mango Waypoint615
Mahogany Waypoint617
Cashew Waypoint621
Cashew Waypoint622
Sugarcane Waypoint625
Sugarcane Waypoint626
Sugarcane Waypoint627
Sugarcane Waypoint628

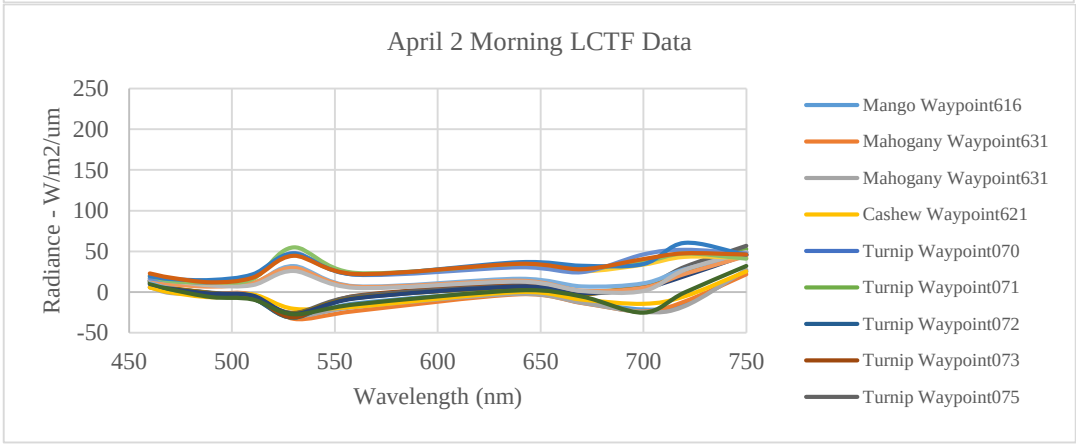
April 2 Morning LCTF Data
Radiance - W/m2/um
250
200
150
100
50
0
-50
450
500
550
600
650
700
750
Wavelength (nm)
Mango Waypoint616
Mahogany Waypoint631
Mahogany Waypoint631
Cashew Waypoint621
Turnip Waypoint070
Turnip Waypoint071
Turnip Waypoint072
Turnip Waypoint073
Turnip Waypoint075

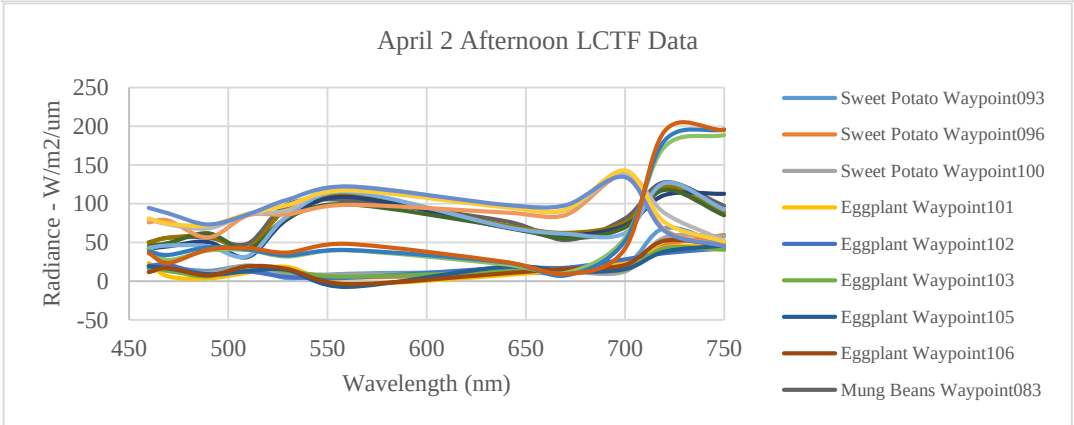
April 2 Afternoon LCTF Data
Radiance - W/m2/um
250
200
150
100
50
0
-50
450
500
550
600
650
700
750
Wavelength (nm)
Sweet Potato Waypoint093
Sweet Potato Waypoint096
Sweet Potato Waypoint100
Eggplant Waypoint101
Eggplant Waypoint102
Eggplant Waypoint103
Eggplant Waypoint105
Eggplant Waypoint106
Mung Beans Waypoint083

Figure 6. LCTF data calibrated to spectral radiance.

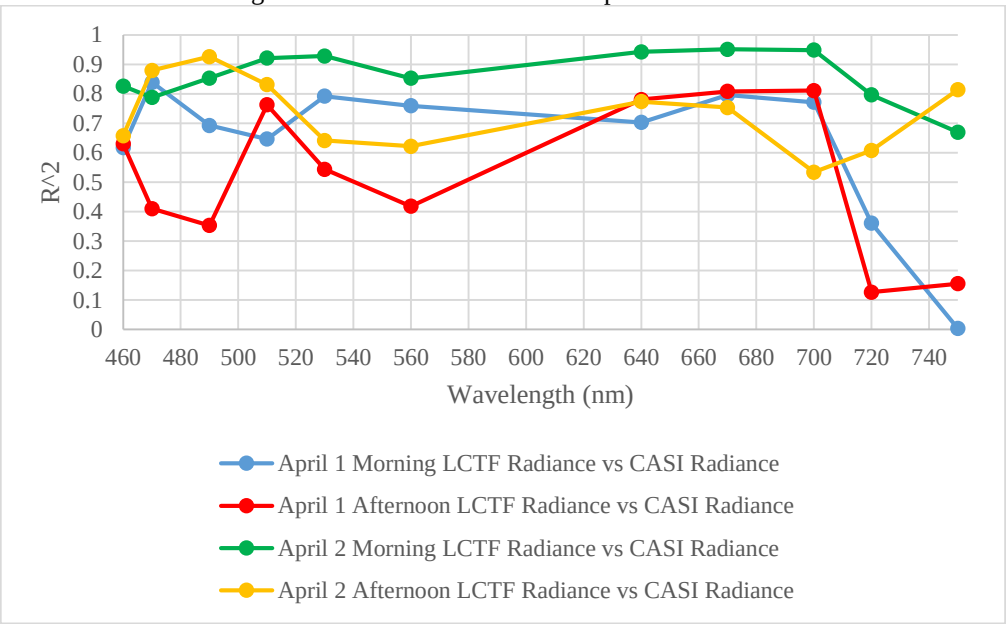

(a)

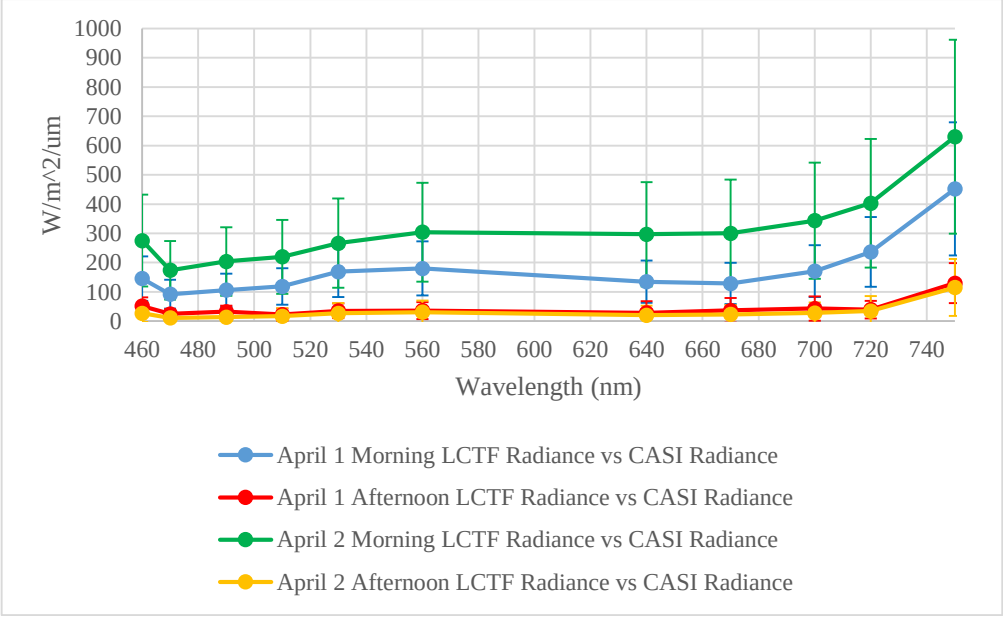

(b)

Figure 7. (a) Linear correlation plots for validation of the calibrated LCTF data compared against CASI data in radiance. (b) Root-mean-square errors of the validation with CASI

5. CONCLUSION

The calibration parameters for the LCTF camera derived on this paper were validated with two other sensors, CASI and FS. The results of the validation displayed a linear correlation coefficient that is 35% to 40% higher in the lower spectrum bands (460 nm to 700 nm) compared to the linear correlation coefficient at the NIR bands (720 nm and 750 nm). The efficacy of the calibration parameters was observed when converting data acquired in the afternoon (2:00 pm to 5:30 pm). If data acquired in the morning (9:00 am to 12:00 nn) were converted into spectral radiance, the RMSE is significantly greater by 200% to 500%.

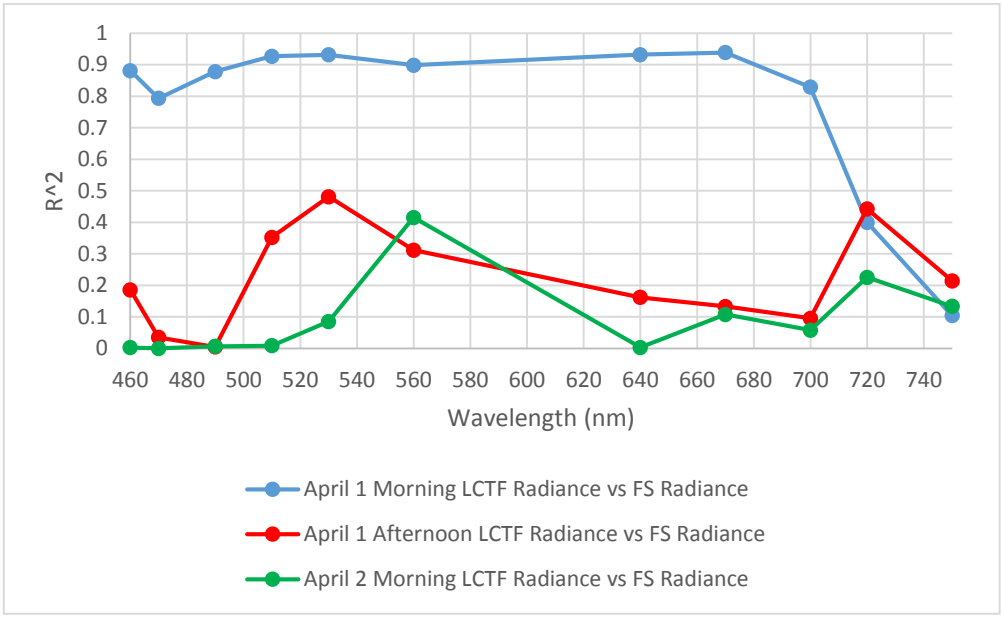

(a)

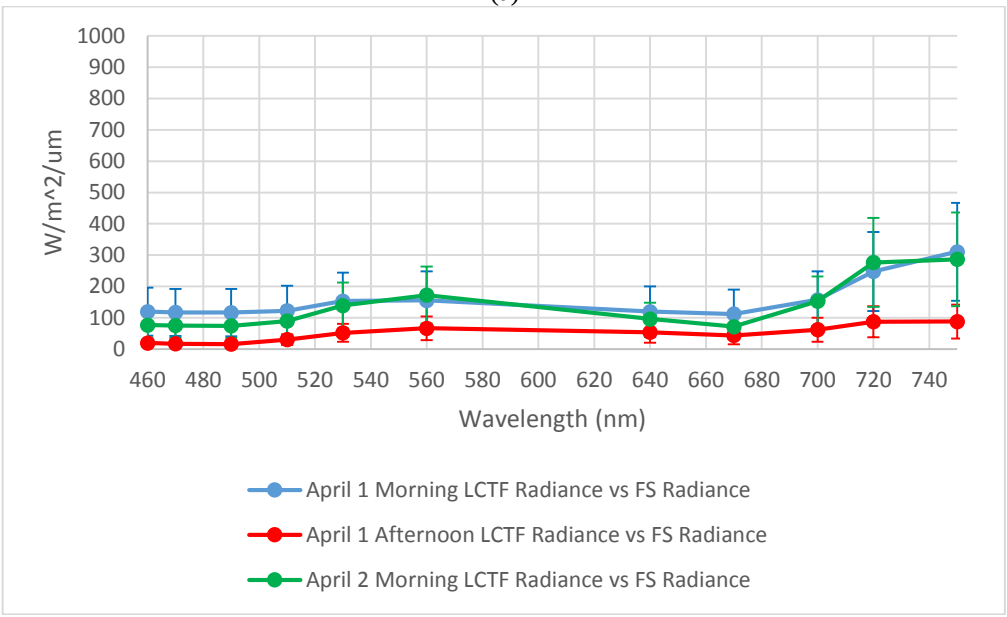

(b)

Figure 8. (a) Linear correlation plots for validation of the calibrated LCTF data compared against FS data in radiance. (b) Root-mean-square errors of the validation with FS

To further improve the calibration and validation in future campaigns, the FS data acquisition should be in radiance so as to eliminate the need of converting from spectral reflectance to radiance. A more diverse collection of target objects is also suggested including different soil types and water bodies.

ACKNOWLEDGMENTS

The experimental airborne mission would not be successful without the assistance of the PHL-MICROSAT Project 5 thru the leadership of Dr. Gay Jane Perez, Chiharu Sasagawa of IHI Corporation, and the service of the Data Acquisition Component of the Phil-Lidar 1 Program.

REFERENCES

1. Bird, R., and Riordan, C., 1984. Simple Solar Spectral Model for Direct and Diffuse Irradiance on Horizontal and Tilted Planes at the Earth's Surface for Cloudless Atmospheres, Solar Energy Research Institute, pp. 2 – 10
2. Dinguirard, M., Slater, P., 1999. Calibration of Space-Multispectral Imaging Sensors: A Review, Remote Sensing of Environment vol. 68 issue 3, pp. 194-205
3. FieldSpec 4 User Manual, 2015, ASD Document 600979, pp. 48 - 69
4. Gat, N., 2000. Imaging Spectroscopy Using Tunable Filters: A Review, The International Society for Optical Engineering SPIE Vol. 4056 pp. 50 - 64
5. ITRES CASI Instrument Manual, 2008, ITRES Research Limited, pp. 26 – 32
6. ITRES Program Data and File Reference, 2007, ITRES Research Limited, pp. 277 – 290
7. Image Processing Correction – Radiometric Correction, Retrieved August 29, 2016 from http://www.jars1974.net/pdf/10_Chapter09.pdf
8. Lopez-Alvarez, M., Hernandez-Andres, J., Romero, J., Campos, J., Pons, A., 2009. Calibrating the elements of a multispectral imaging system, Journal of Imaging Science and Technology 53(3): 031102-031102-10
9. Nouri, D., Lucas, Y., Treuillet, S., 2013. Calibration and test of a hyperspectral imaging prototype for intra-operative surgical assistance, Proc. SPIE 8676, Medical Imaging 2013, pp. 8670P
10. Peddle, D., White, P., Soffer, R., Miller, J., LeDrew, E., 2000. Reflectance processing of remote sensing spectroradiometer data, Computer & Geosciences 27 (2001) pp 203 – 213
11. Radiometric Corrections, Retrieved August 29, 2016 from http://gsp.humboldt.edu/olm_2015/Courses/GSP_216_Online/lesson4-1/radiometric.html
12. Radiometric Correction of Satellite Images: When and Why Radiometric Correction is Necessary, Retrieved August 29, 2016 from http://www.ncl.ac.uk/tcmweb/bilko/module7/lesson3.pdf
13. Saito, G., Seki, H., Uto, K., Kosugi, Y., Komatsu, T., 2014. Development of hyperspectral imaging sensor, which mounted on UAV for environmental study at coastal zone, OS-083 ACRS2014
14. Sakamoto, Y., Gonzalez, A., Espiritu, J., Labrador, J., Oliveros, J., Kuwahara, T., Yoshida, K., 2015. Development of the Satellite Bus System for PHL-MICROSAT. Japan Geoscience Union Meeting MTT06-04
15. Slater, P., Biggar, S., Holm, R., Jackson, R., Mao, Y., Moran, M., Palmer, J., Yuan, B., 1987. Reflectance and radiance-based methods for the in-flight absolute calibration of multispectral sensors, Remote Sensing of Environment vol. 22 issue 1, pp. 11- 37
16. Thome, K., 2001. Absolute radiometric calibration of Landsat 7 ETM+ using the reflectance-based method, Remote Sensing of Environment vol. 78 issues 1-2, pp. 27 - 38
17. Vergel, K., Magallon, B., Takahashi, Y., Ishida, T., Perez, G., Tupas, M., Marciano, J., 2015. Science Missions and Payloads of Philippines' First Earth Observation Microsatellite: Diwata